A MINIATURE HIGH-SENSITIVITY BROAD-BAND ACCELEROMETER BASED ON ELECTRON TUNNELING TRANSDUCERS

Howard K, Rockstad, T. W. Kenny, J. K. Reynolds,
W. J. Kaiser, and Thomas B. Gabrielson*

Jet Propulsion Laboratory
Center for Space Microelectronics Technology
California Institute of Technology
Pasadena, California 91109-8099
*Naval Air Warfare Center
Warminster, Pennsylvania 18974-0591

ABSTRACT

New high-sensitivity microsensors have been developed using high-resolution position sensors based on electron tunneling. Design of miniature accelerometers having sensitivities approaching 10-9 $g/\sqrt{Hz}$ is discussed, A new dual-element electron tunneling structure, which overcomes bandwidth limitations of single-element structures, allows design of high sensitivity accelerometers operating in a band from a few Hz to several kHz. A miniature accelerometer based on this structure can thus have application as a sensitive acoustic sensor. Thermal vibration of the proof mass is an extremely important constraint in miniature accelerometers, and can be the dominant limitation on the sensitivity. Thermal noise is analysed for the suspended masses of the dual-element structure, and compared with electronic noise in the tunneling circuit. With a proof mass of 100 mg, noise analysis predicts limiting sensitivities approaching 10-9 $g/\sqrt{Hz}$ in a 300 Hz band and 10^{-8} $g/\sqrt{Hz}$ at 1 kHz. Prototype accelerometers have been fabricated by silicon micromachining and tested, Sensitivity better than 10^{-6} $g/\sqrt{Hz}$ at 10 Hz is obtained in a heavily damped device tested in air; a Q>>1 is obtained in vacuum, and is expected to give much improved sensitivities,

INTRODUCTION

Advances in microelectronics and silicon micromachining have enabled the convenient fabrication of compact structures, providing new capabilities for producing new sensors and instruments. However, the development of compact sensors has been constrained by a variety of fundamental sensor sensitivity limits. In particular, the development of compact sensors for many of the most important applications often requires a drastic improvement in displacement transducer detection sensitivity. Thus, new fabrication techniques may not, alone, yield suitable microsensors. Recent developments at JPL, based on novel signal detection principles, have produced a series of ultra-high sensitivity microsensors and microinstruments. Included among the applications demonstrated are a micro-seismometer, micro-accelerometer, micro-magnetometer, and a unique uncooled infrared detector. Several of these sensors utilize

electron tunneling as an ultrasensitive displacement sensor [1-4]. For example, this method has been described by Kenny, *et al.* [2-4] in the development of sensitive uncooled infrared detectors. High sensitivity in a compact detector without the need for cryogenic cooling is a major advantage of this Golay cell infrared detector. Another application of electron tunnel sensors, which is the subject of this paper, is in sensitive, compact, accelerometers capable of detecting accelerations of the order of 10-9 to 10^{-8} $g/\sqrt{Hz}$. Such accelerometers can be used in a band from several Hz to several kHz, and can have application as sensitive acoustic sensors. Growing needs for small, low-cost accelerometers include hydrophore networks for monitoring of oceanic activity.

Miniature accelerometers have been described by numerous authors[4- 10]. Some miniature accelerometers are intended for fairly large forces, such as those encountered in automotive applications for air bag deployment. Other applications require sensitivity to extremely small signals, and in this regime Rudolf [8] has described a capacitive accelerometer with micro-g resolution at 1Hz. Accelerometers function by employing proof masses whose motion responds to accelerations. Motion of the proof mass relative to the accelerometer case is measured and converted to motion of the case. Significantly better resolution requires different approaches, such as electron tunneling, for measuring displacement of the proof mass.

Displacement transducers based on electron tunneling have been shown by Waltman and Kaiser [1] and by Kenny, *et al.* [2] to offer high sensitivity, approaching 10^{-4} Å/$\sqrt{Hz}$ at 10 kHz. Employing a tip similar to those used in Scanning Tunneling Microscopy (STM), Waltman and Kaiser observed an acceleration resolution of 10^{-5} $g/\sqrt{Hz}$ with a bandwidth of 3 kHz. A prototype micromachined silicon tunneling accelerometer utilizing a micromachined silicon tip coated with gold gave an inferred acceleration resolution of 5 x 10-8 $g/\sqrt{Hz}$ at 10 Hz [2]. However, stable operation of the feedback circuit was limited to frequencies below the suspended proof mass natural frequency of 225 Hz.

Electron Tunneling Displacement Transducers

Operation of a tunnel tip in an STM mode is illustrated in Refs. 1-4. A tunnel current I is established between a tip and a counterelectrode by a small bias voltage V. In typical STM operation, feedback circuitry controls the vertical position of the tip by means of a piezoelectric transducer so as to maintain the tunnel current constant, thereby also maintaining the electrode spacing s constant, while the specimen is scanned laterally. Tunnel current I depends on electrode spacings as [11]

$$I \propto Ve^{-\alpha\sqrt{\Phi}s} \quad (1)$$

where $\alpha = 1.025\,\text{Å}^{-1}\text{eV}^{-1/2}$ is the height of the tunnel barrier, and the bias voltage V (typically about 200 mV) is small compared to Φ. For typical values of Φ and s (0.5 eV and 10 Å, respectively), the current varies by a factor of two for each Å change in electrode separation, Because of this extreme sensitivity to position, the tip-to-substrate separation is maintained constant to high precision, The output of the feedback circuitry is used as a measure of the tip's vertical separation in the illustration. The tunnel transducer's sensitivity to

position is superior to that of other compact transducers, and is orders of magnitude better than standard compact capacitive sensors. The sensitivity of a tunnel transducer is independent of device size, because of the extremely small size of the tunneling tip, in contrast with a capacitive sensor, for example. Thus, miniaturization of the transducer causes no reduction in sensitivity,

DUAL-ELEMENT TUNNEL ACCELEROMETER

The tunnel accelerometer described by Kenny, et al, [2] comprises a single suspended mass component, the proof mass. Electron tunneling takes place between a tip on the proof mass and a fixed counterelectrode on the case. Operation of this accelerometer uses electronic feedback circuitry to maintain a constant tip-to-counterelectrode spacing, as in scanning tunneling microscopy, by controlling an electrostatic deflection voltage on the suspended mass. When the sensor is accelerated, the proof mass experiences an inertial force which causes it's motion to lag that of the sensor. The feedback circuit generates an electrostatic re-balance force which causes the proof mass to follow the motion of the sensor, Stable operation is restricted to frequencies below the natural frequency of the proof mass, 225 Hz in this case.

Fig. 1, Schematic illustration of a micromachined dual-element electron tunneling accelerometer. The boron-doped epitaxial silicon layer is used for the wide-bandwidth cantilever.

Many applications require a larger bandwidth. To overcome the frequency limitations of the single-element system, a new dual-element system has been designed, as illustrated in Fig. 1. This design separates the proof mass and the electrical transducer so that their mechanical properties can be independently tailored. Tunneling occurs between electrodes on a wide-bandwidth cantilever and on the proof mass, The wide-bandwidth cantilever is controlled electrostatically by high-frequency feedback circuitry to closely follow the motion of the proof mass, Since the proof mass may have a low resonant frequency, it's dynamics may be tuned to enhance acceleration sensitivity. An optional low-frequency secondary feedback circuit maintains the mass position within suitable range of the cantilever, The output signal of the transducer is derived from the high-frequency feedback circuitry, as illustrated in Fig. 2. This signal has bandwidth > 10 kHz, and the dynamic range above the noise floor of the transducer is > 100 dB.

Fig. 2. Tunnel transducer feedback circuitry.

THEORY

Fig. 3. Schematic illustration of a two-mass system with spring constands k_p and kc and damping coefficients R_p and R_c.

Performance of a sensor system depends on noise sources inherent within the system as well as on the responsivity of the system. As has been described by Gabrielson [12] and is shown in the following analysis, thermal vibration of the proof mass is an extremely importan consideration of a high-sensitivity miniature accelerometer. Noise sources are analysed here for a dual-element design, represented by the mass-suspension system in Fig, 3. The proof mass m_p and cantilever mass m_c are suspended independently from the frame with spring constants k_p and kc, and with damping coefficients R_p and R_c. The relations between the mass motions and the frame motion can be obtained by solving the equations of motion when the frame is subjected to a sinusoidal driving force. From the steady-state solutions for each mass, the relations between the rms amplitude Y of the frame motion and the rms amplitudes Z_p and Z_c for the masses relative to the frame are

$$Z_c = \frac{Y\Omega_c^2}{\sqrt{(1-\Omega_c^2)^2 + \frac{\Omega_c^2}{Q_c^2}}} \quad \text{and} \quad Z_p = \frac{Y\Omega_p^2}{\sqrt{(1-\Omega_p^2)^2 + \frac{\Omega_p^2}{Q_p^2}}} \tag{2}$$

where $\Omega_p = \omega/\omega_{op}$, $Q_p = m_p\omega_{op}/R_p$, $\Omega_c = \omega/\omega_{oc}$, and $Q_c = m_c\omega_{oc}/R_c$.

From the relative displacement $z \equiv z_c - z_p$ of the two independently-suspended masses, the rms amplitude of relative motion is

$$Z(rms) = \sqrt{Z_c^2 + Z_p^2 - 2Z_cZ_p\cos(\phi_c - \phi_p)} \tag{3}$$

where

$$\phi_c = \tan^{-1}\frac{\omega\omega_{oc}}{(\omega_{oc}^2 - \omega^2)Q_c} \quad \text{and} \quad \phi_p = \tan^{-1}\frac{\omega\omega_{op}}{(\omega_{op}^2 - \omega^2)Q_p} \tag{4}$$

The transfer function between the measured motion Z and the desired frame motion Y is given by Eqns. 2-4, The frequency range of interest is $\omega << \omega_{oc}$, that is, frequencies less than the natural frequency of the cantilever. By design, the proof mass natural frequency is small compared to the cantilever natural frequency, so $\Omega_c << \Omega_p$ and, accordingly, $Z_c << Z_p$. Thus, in the band of interest, the **transfer function is** approximately

$$Z \approx \frac{Y\Omega_p^2}{\sqrt{(1-\Omega_p^2)^2 + \frac{\Omega_p^2}{Q_p^2}}} \quad (5)$$

The suspended masses are subject to thermal noise [12],which may be included in the equation of motion as a force $F(\mathrm{rms}) = \sqrt{4k_BTR}\ \mathrm{N}/\sqrt{\mathrm{Hz}}$; this is the N yquist relation for a mass-spring oscillator with damping coefficient R. The steady-state solutions for thermal noise at frequency ω are oscillations with rms amplitudes

$$Z_{np} = \sqrt{\frac{4\,k_B\,T}{\omega_{op}k_pQ_p[(1-\Omega_p^2)^2 + \frac{\Omega_p^2}{Q_p^2}]}}$$

(6)

$$Z_{nc} = \sqrt{\frac{4\,k_B\,T}{\omega_{oc}k_cQ_c\,[(1-\Omega_c^2)^2 + \frac{\Omega_c^2}{Q_c^2}]}}\,.$$

Using Eq. 5, the *frame-equivalent* rms noise terms are

$$Y_{np} \approx \frac{1}{\omega^2}\sqrt{\frac{4\, k_B\, T\, \omega_{op}}{m_p\, Q_p}} \quad \text{and} \quad Y_{nc} \approx \frac{1}{\Omega_p^2}\sqrt{\frac{4\ k_B\, T[(1-\Omega_p^2)^2 + \frac{\Omega_p^2}{Q_p^2}]}{\omega_{oc} k_c Q_c\, [(1-\Omega_c^2)^2 + \frac{\Omega_c^2}{Q_c^2}]}} \tag{7}$$

where the subscripts c and p refer to parameters of the cantilever and the proof mass,

From the shot noise expression $I_n = \sqrt{2eI}$ Amps / $\sqrt{\text{Hz}}$, coupled with the tunnel current relation, the frame-equivalent shot noise in the tunnel current I is

$$Y_{ns} \approx \frac{1}{\Omega_p^2}\ \sqrt{\frac{2e}{I\Phi\alpha^2}}\ \sqrt{(\ (1-\Omega_p^2)^2 + \frac{\Omega_p^2}{Q_p^2})} \tag{8}$$

where Φ and α were defined earlier for the tunnel tip. Johnson noise in the tunneling process arises from the zero-bias interchange of electrons across the gap, and is independent of bias. For a tunnel current of 1 nA at a tip bias of 100 mV, the frame-equivalent Johnson noise is 0,7 times the shot noise given by Eq. 8. Johnson noise at the first resistor in the electronic circuit, typically 10 MΩ, is a factor of 4 less than the tunnel current shot noise. Because of the large responsivity of the tunnel transducer, amplifier noise is unimportant,

An important conclusion from Eq. 7 is that proof mass thermal noise equivalent displacement is proportion to $\sqrt{f_o / mQ}$. Thermal noise equivalent acceleration of the case at frequency ω is readily obtained from the product of ω^2 and the noise equivalent case displacement,

Fig. 4. Thermal noise equivalent case acceleration for various noise sources including thermal vibration of two masses and shot noise in the electron tunneling current.

Theoretical thermal noise equivalent case accelerations are shown in Fig. 4 for a 100 mg proof mass with a 100 Hz natural frequency and a 9 microgram cantilever with a 16 kHz natural frequency. A Q of 200 has been taken for both elements. Actual Q values are expected to be much higher. Shot noise is calculated for a tunnel current of 1 nA. As the figure shows, for these parameters, thermal noise in the proof mass dominates for a band of several hundred Hz. Thermal noise from the cantilever mass is comparable in magnitude to shot noise and Johnson noise and above several hundred Hz

they dominate, increasing as f^2. The noise equivalent acceleration of about 2x10-8 $g/\sqrt{Hz}$ illustrated in the figure corresponds to a proof mass relative motion of 5 x 10-4 Å, which tunneling transducers are capable of measuring [4]. Thus, it can be concluded that it is possible to construct an accelerometer with a proof mass as small as 100 mg which can detect signals of the order of 10-9 $g/\sqrt{Hz}$. According to Eq. 8, the low frequency thermal noise can be reduced by increasing mQ/fo; thus, larger mQ product and smaller f_0 can be utilized to improve performance. Q >1 introduces a peak in the Z/acceleration transfer function at the proof mass resonance. If this peak is in the frequency band of interest, and particularly if Q is large, techniques to accommodate it may be utilized. Such techniques include straightforward signal processing or utilization of a pair of detectors with different resonant frequencies for each axis of motion. Alternatively, for very large Q it may be suitable to block a narrow frequency band encompassing the peak.

This analysis also shows the difficulties encountered in fabricating sensitive accelerometers with extremely small proof masses in the microgram range. For example, for a proof mass of 1 microgram and a Q of 1000, the thermal noise equivalent acceleration from Eq. 7 is 3×10^{-6} and 10-5 $g/\sqrt{Hz}$ for natural frequencies of 10 and 100 kHz, considerably higher noise than the noise floors and acceleration sensitivities discussed in this paper. In addition, as the natural frequencies for very small proof mass systems may be expected to be high relative to the 100 Hz assumed for Fig. 4, the limiting resolution of the displacement transducer must be correspondingly better in order to measure the smaller proof mass motions.

EXPERIMENTAL

We have constructed and tested a prototype dual-element accelerometer of micromachined silicon with a 50 mg proof mass. As illustrated schematically in Fig. 1, the proof mass is suspended from a silicon spring on one end. The high-frequency cantilever is 4 microns thick and 0.7 mm long, and comprises boron-doped Ge-alloyed silicon, Ge alloying is chosen to compensate for the heavy boron doping in order to give a low-stress cantilever. External chip dimensions are 13 mm x 13 mm. Initial tests, described in this paper, were conducted in air. Subsequent tests are being conducted in vacuum. Vibration tests were conducted with the test device and a calibrated Kistler Model 808KT108 accelerometer mounted side-by-side on a massive metal plate. The plate was excited sinusoidally, and signals from both accelerometers were measured on a Hewlett-Packard Model 3582A spectrum analyser. The silicon mass chip was suspended vertically, and the mounting plate was vibrated horizontally. Measurements were performed for a number of frequencies from 5 Hz to 3 kHz. At selected frequencies, the vibration amplitude was varied and linearity tests were made. The responsivity is large, being about 20 mV for 10^{-5} g acceleration at 10 Hz, for example. As shown by Fig. 5, the signal from the tunnel accelerometer is extremely linear, as expected, given the design of the suspension and the nature of the force rebalance mode of operation. The noise floor at 10 Hz corresponds to 6 x 10-7 $g/\sqrt{Hz}$ and increases to 10-5 $g/\sqrt{Hz}$ at 1 kHz. As the Q for this test was very low (Q<<1) due to the air surrounding the suspended components, the responsivity is expected to increase and the noise floor is

expected to decrease markedly when vibration tests are conducted in vacuum, where the device exhibits $Q>>1$.

Devices have been fabricated both with and without shaped silicon tips. The data of Fig. 5 are obtained from a device with no protruding tip of that form, relying on the fact that tunneling will take place between the nearest atoms, so that a sharp tip is not essential. In this case the high-frequency cantilever is triangular in order to limit the region of nearest approach for tunneling,

Fig. 5. Tunnel accelerometer output vs. calibrated accelerometer output at 100 Hz, illustrating the linearity of the tunnel accelerometer.

CONCLUSION

Electron tunneling displacement transducers offer extremely high resolutions which can be utilized for sensitive microinstruments. A new dual-element micromachined silicon tunnel accelerometer which extends the operational bandwidth beyond the resonant frequency of the proof mass has been successfully fabricated and demonstrated. The dual-element design, comprising a low-resonant-frequency proof mass oscillator and a high-frequency tunnel transducer cantilever, provides flexibility for independently optimizing the proof mass oscillator and the tunnel transducer, In a heavily damped system with $Q<<1$, the responsivity is large, being 20 mV for a 10-5 g acceleration at 10 Hz. The noise floor for the same system is 6 x 10-7 $g/\sqrt{Hz}$ at 10 Hz. Both responsivity and noise floor are expected to improve when a larger Q is obtained by evacuating the device. Thermal noise analysis is essential for microaccelerometers with smal l proof masses. Anal ysis for a system with a 100 mg proof mass and a proof mass resonant frequency of 100 Hz shows that the dominant noise source is thermal noise of the suspended masses. Electronic noise for an electron tunnel transducer is less. This noise anal ysis shows that compact accelerometers with proof masses in the range of 100 mg are capable of measuring signals significantly less than 10^{-6} g; Qs greater than 1 are necessary to sense nano-g signals. For a 100 mg proof mass, a 100 Hz resonant frequency, and a Q of 200, an acceleration resolution approaching 10-9 $g/\sqrt{Hz}$ in a 300 Hz band and 10-8 $g/\sqrt{Hz}$ at 1 kHz are predicted for the dual-element device. Electron tunnel sensors are necessary for these high resolutions in such a small device.

ACKNOWLEDGMENTS

The research described in this paper was performed by the Center for Space Microelectronics Technology, Jet Propulsion Laboratory, California Institute of Technology, and was jointly sponsored by Naval Air Warfare Center, Strategic Defense Initiative Organization/innovative Science and Technology Office, and Defense Advanced Research Projects Agency. The authors are grateful to T. R. VanZandt for suggestions and discussion,

REFERENCES

[1] S. B. Waltman and W. J. Kaiser, "An Electron Tunneling Sensor," Sensors and Actuators, vol. 19, pp. 201-210, 1989.

[2] T. W. Kenny, S. B. Waltman, J. K. Reynolds, and W. J. Kaiser, "A Micromachined Silicon Electron Tunneling Sensor," Proc. IEEE Micro Electro Mechanical Systems Conference, Napa Valley, CA, U.S.A, February 11-14, 1990, pp. 192-196; ibid., "Micromachined Silicon Tunnel Sensor for Motion Detection," Appl. Phys. Letters, vol. 58, pp. 100-102, 1991.

[3] T. W. Kenny, W. J. Kaiser, S. B. Waltman, and J. K. Reynolds, "Novel Infrared Detector Based on a Tunneling Displacement Transducer," Appl. Phys. Letters, vol. 59, pp. 1820-1822, *1991.*

[4] T. W, Kenny, W. J. Kaiser, J. K. Reynolds, J. A. Podosek, H, K. Rockstad, E. C. Vote, and S. B. Waltman, "Electron Tunnel Sensors," J. Vat. Sci. Technol., vol. A 10, pp. 2114-2118, 1992.

[5] W. D. Frobenius, S. A, Zeitman, M, H. White, D, D, O'Sullivan, and R, G. Hamel, "Microminiature Ganged Threshold Accelerometers Compatible with Integrated Circuit Technology," IEEE Trans. Elect, Devices, vol. ED-19, p. 37, 1972.

[6] L. M. Roylance and J. B. Angell, "A Batch-Fabricated Silicon Accelerometer," ibid., vol. ED-26, pp. 1911-1917, 1979.

[7] K. E. Petersen, A. Shartel, and N. F. Raley, "Micromechanical Accelerometer Integrated with MOS Detection Circuitry," ibid., vol. ED-29, pp. 23-27, 1982.

[8] F. Rudolph, "Precision Accelerometers with μg Resolution," Sensors and Actuators, vol. A21-A23, pp. 297-281, 1990.

[9] D. W. de Bruin, H. V, Allen, S. C. Terry, "Second-order Effects in Self-testable Accelerometers," Technical Digest of the IEEE Solid State Sensor and Actuator Workshop, Hilton Head, SC, U. S. A., June, 1990 pp. 149-152.

[10] W. Henrion, L. DiSanza, M. Ip, S. Terry, and H, Jerman, ibid., p. 153,

[11] G. Binnig and H. Rohrer, IBM J. Res. Develop. 30, 355 (1 986).

[12] T. B. Gabrielson, "Mechanical-thermal Noise in Micromachined Acoustic and Vibration Sensors," IEEE Trans. Electron Devices, May, 1993.

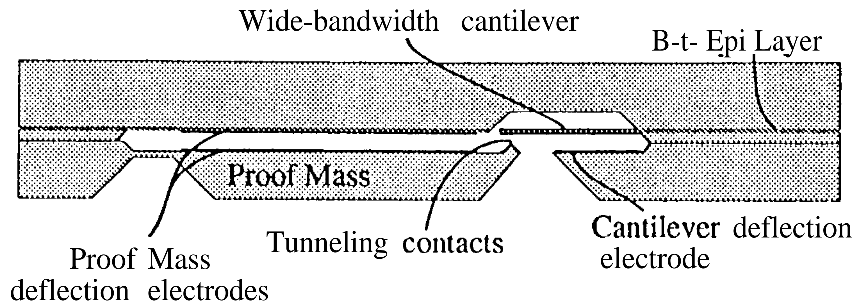

Fig. 1

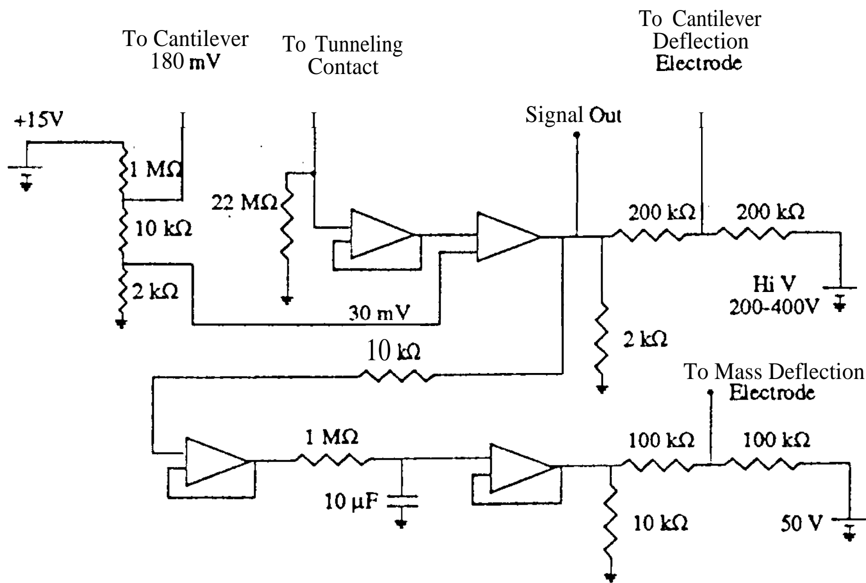

Fig. 2

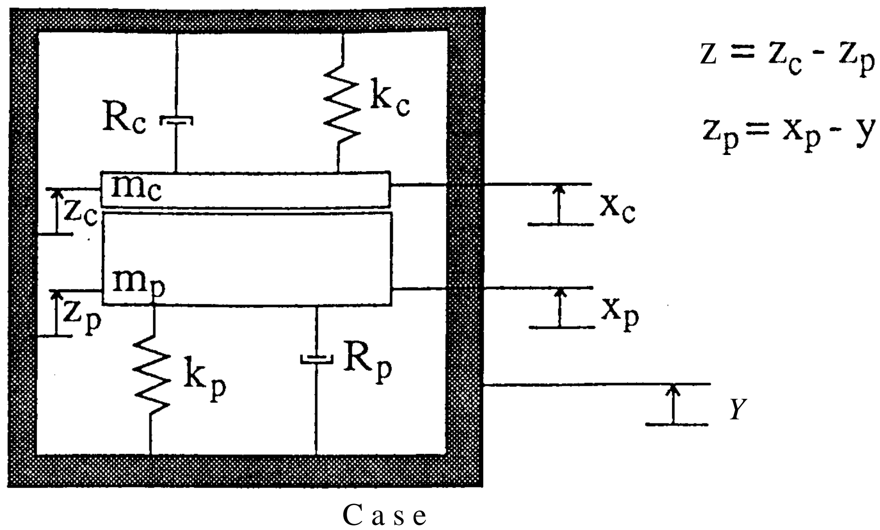

$$z = z_c - z_p$$

$$z_p = x_p - y$$

Fig. 3

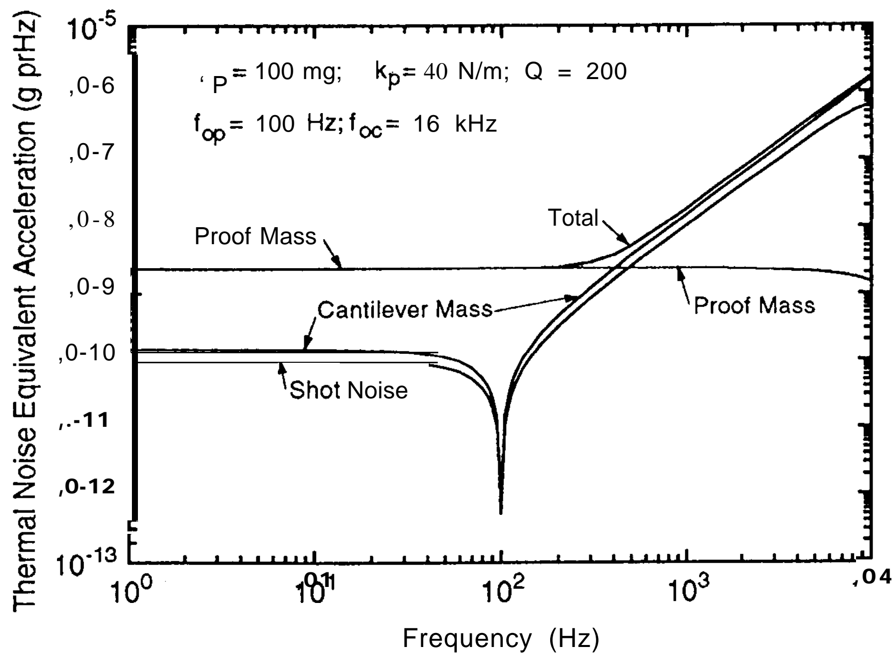

Fig. 4

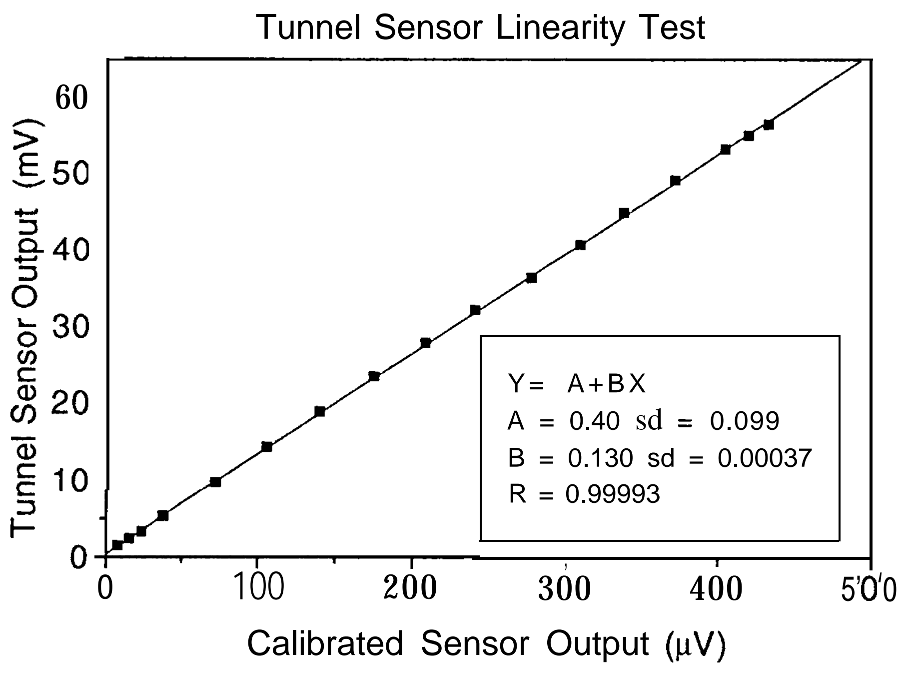

Fig. 5